Report to the Radar Operations Center

Covering Work Done Under Memorandum of Understanding with the Office of Hydrologic Development

July 2005-May 2006

July 31, 2006

David Kitzmiller, Dennis Miller, and Kiran Shrestha

Hydrology Laboratory
Office of Hydrologic Development
National Weather Service, NOAA

TABLE OF CONTENTS

Executive Summary

This report documents results and progress in an ongoing analysis of dual-polarization radar precipitation estimation algorithms developed by the National Severe Storms Laboratory (NSSL). Our goal is to determine the degree to which these algorithms improve upon the accuracy of existing horizontal polarization algorithms operational within the WSR-88D system. Results can be summarized as follows:

Evaluation of the "Combined" multi-algorithm rainfall estimation algorithm:
This algorithm represents a synthesis of horizontal- and dual-polarization algorithms based on reflectivity, differential reflectivity, and specific differential phase. A description was presented by Ryzhkov et al. in April 2006; Office of Hydrologic Development staff obtained estimates from this Combined algorithm for several historic cases in May 2006. Our analysis indicates that in terms of 1-hour rainfall amounts, the Combined algorithm yields estimates of about the same accuracy as a Z-R algorithm, but with higher absolute accuracy in heavy rainfall > 0.1 inch h^{-1}. Visual inspection of the data sample provided by NSSL shows that components of the precipitation algorithm introduce random noise, and radar-gauge correlation is improved by spatial filtering through a consensus-average algorithm.

Evaluation of the dual-polarization algorithm as applied to S-band dual-polarization observations over Florida:
Because much recent analysis of the NSSL algorithms has been focused on the storm environment of Oklahoma, we wished to verify that these algorithms function effectively in other areas. Therefore we have analyzed the output of the NSSL "Synthetic" algorithm (functionally similar to the later "Combined" algorithm) as applied to data collected with the NCAR S-pol radar when it was deployed in Melbourne, Florida in 1998. Here, results were consistent with those from Oklahoma; detection of rainfall and the spectrum of rainfall values were similar to those from the nearby operational WSR-88D unit. As has been noted by both NCAR and NSSL scientists, the specific differential phase (Kdp) part of the algorithm is highly sensitive to the methods used to compute it, and further work is needed to make the Kdp-based rainrate estimates statistically stable.

Evaluation of the Hydrometeor Classification Algorithm (HCA) as a filter for airborne non-precipitation echoes
The currently-operational Radar Echo Classifier has little effect in identifying aerial targets such as migrating birds and insects, which produce an echo spectrum similar to light stratiform precipitation. Consequently, a cloud of light precipitation often appears in a roughly circular pattern around WSR-88D sites, particularly during the spring migration season. We examined a set of cases with mixed precipitation and bird echoes, and verified that the HCA does indeed have the ability to consistently identify and remove return from birds. It is possible that the addition of a final step to remove speckle or "shot noise" echoes may further improve results. While an enhanced horizontal-polarization Precipitation Detection Algorithm might be capable of eliminating these extraneous accumulations, the implementation schedule is such that dual-polarization techniques might be available in nearly the same timeframe.

The effects of "beam-splitting" on precipitation detection

The current design of the dual-polarization upgrade to the WSR-88D requires simultaneous transmission of horizontally- and vertically-polarized microwaves. This "beam-splitting" technique has the effect of slightly reducing the sensitivity of the radar by about 3 dB. Initial analysis by NSSL and CIMMS indicated this should have little effect on most operational Doppler-based products. An initial assessment based on a comparison of collocated WSR-88D and dual-polarization radar data is illustrated here. Indications are that the sensitivity loss has little impact at close ranges, though there is the possibility that the different hardware or algorithm differences may cause differences in precipitation detection at longer ranges.

Summary of items for future action by NSSL and OHD:

Verify that proposed NSSL modifications to Kdp estimation do, in fact, eliminate or substantially reduce apparent noise in rainfall estimates;

Study potential modification to HCA, or post-processing of HCA output, to more realistically portray regions near the radar with biological targets;

Carry on with study of the effects of sensitivity degradation;

Provide a test plan for a preproduction dual-polarization WSR-88D to be deployed in a cooler, more humid environment than Oklahoma, to better examine dual-polarization estimates in stratiform precipitation.

I. Initial Evaluation of the NSSL Dual-Polarization "Combined" Algorithm

In May 2006, NSSL staff briefed the NEXRAD Software Recommendation and Enhancement Committee on results from a new form of the Synthetic algorithm (referred to hereafter as the "Combined" algorithm. We received a new sample of precipitation algorithm estimates shortly afterwards.

Our aim was to evaluate the characteristics of the dual-polarization "Combined" algorithm described by Ryzhkov (2006). NSSL staff provided a sample of 90 hours' data over 6 calendar days in 2004-2005. We collated these 1-h, 2-km precipitation estimates from the dual-polarization Combined algorithm with Z-R estimates also derived from the KOUN research dual-polarization radar, contemporaneous estimates from the KTLX (Twin Lakes) WSR-88D unit, and rain gauge reports from the Oklahoma Mesonet. Mesonet observations from 119 sites were obtained from the Oklahoma Climate Survey's web site. These appear to be of superior quality to observations from the HADS archive, which receive less quality control; the correlation between the Mesonet observations and all the radar observations was higher than the correlation between the HADS data and radar.

To assess the general precision of the Combined algorithm and the likelihood of its providing good operational continuity with the existing WSR-88D algorithm, we compared rain gauge to radar estimates in terms of rank correlation and root-mean-squared (RMS) error, for several subsets of the data. We also examined the precipitation "coverage" bias by determining the percentages of gauge and radar reports with measurable ($\geq$ 0.01 in) rainfall.

We include operational estimates from KTLX primarily as a reference for general skill level. Since this radar unit is in constant use and undergoes routine maintenance, it's likely that its overall calibration is superior to that of KOUN, which served as an engineering testbed during much of the study period to date. These circumstances would enable KTLX to provide products statistically superior to those from KOUN; we can expect some improvement in dual-polarization products with fully operational radar units.

Test cases

Sample 1-h rainfall estimate fields from each of the study events are shown in Figs. 1-5. The events can be characterized as follows:

21 April 2004:	convective rainfall with some hail
3 June 2004:	convective and stratiform rainfall
9-10 June 2004:	primarily convective rainfall
15 November 2004:	stratiform rain with bright-band enhancement
6 February 2005:	stratiform rain with bright-band enhancement

General characteristics of the Combined algorithm output

The precipitation estimates are presented on a 2-km Cartesian grid nearly centered on the radar site. Figs. 1-5 show the Combined algorithm estimates (top image in each figure) and Z-R

estimates based on the convective relationship $Z=300R^{1.4}$ (lower image). The areal coverage and overall distribution of 1-hour Combined estimates are similar to those of the Z-R estimates. However, the Combined estimates in their present form appear "noisier" and have some zero-value bins scattered throughout most of the heavier precipitation areas. These dropouts are usually due to instabilities with Kdp calculations (Ryzhkov, personal communication; Scott Ellis, personal communication).

In convective areas (Figs. 1-3) it appears that the combined algorithm generally lowers the highest amounts indicated by the Z-R estimates. Note particularly the higher accumulations in the mesoscale line immediately east of the radar, and the isolated cell northwest of the radar, in Fig. 1. These accumulations exceed 1.5 inch in some areas, but the Combined algorithm lowers the peak values to 1 inch or less.

For both cool-season events (Figs. 4,5) there is a suggestion of bright-band enhancement. This version of the Combined algorithm attempts to apply the Kdp-based estimates in areas where the radar beam detects melting snow. This had minimal effect in mitigating the apparent overestimation. Future versions of the algorithm will estimate precipitation under the bright band by applying the standard Z-R relationship adjusted downward by a factor of 2 (Ryzhkov 2006).

Statistical characteristics of the Combined Algorithm estimates

The Combined algorithm output for 1-h amounts was collated with Z-R estimates from the KOUN unit, Z-R estimates from the KTLX WSR-88D unit at Twin Lakes, and with rain gauge reports from the Oklahoma Mesonet. During most hours the nominal ending times did not fall at precisely the top of the hour; in such cases temporal interpolation was used to estimate the hourly accumulation valid at the top of the hour. For each rain gauge site, the radar rainfall from both the 2-km grid box containing the gauge location, and an average rainfall for the 4-km region centered closest to the gauge (4 2-km grid boxes), were paired with the gauge value. One-hour WSR-88D estimates from the KTLX unit were taken from Digital Precipitation Array (DPA) products, which have a grid mesh of ~4 km over Oklahoma. Hereafter these are referred to as the COMB, COMB 4KM, Z-R, Z-R 4KM, and DPA radar estimates.

The collating process yielded 4787 gauge-radar pairs, of which 4075 had measurable precipitation indicated by at least one of the sensors (the high fraction being due to pre-selection of precipitation events). Of this set, 1901 radar-gauge pairs were within 120 km of the KOUN unit, hereafter referred to as the "nearby" subset.

Both KOUN and KTLX appear to detect somewhat fewer rain events than is indicated by the Mesonet gauges, over both the entire umbrella and within the innermost 120 km, as shown in Fig. 6. There is little bias between the two radars, and between the two KOUN algorithm estimates, in terms of total precipitation area, with both units indicating about 23% coverage overall and 33% in the inner umbrella; the gauge network indicated 35% and 38% over the two respective domains.

Likewise, both radars and both KOUN algorithms have similar information with respect to rain gauge reports, in terms of rank correlation coefficient (Fig. 7). The rank correlation is the linear correlation between rank positions of two sets of variables. We applied this statistic, rather than linear correlation, in order to better judge the information inherent in the radar data,. The linear correlation is affected not only by the amount of predictive information in the radar but by the degree of linearity in the radar-gauge relationship.

Since this data sample features both precipitation and nonprecipitation areas, some of the information comes from rain/no-rain discrimination and some from correlation with rainfall amount. The correlation is distinctly higher in the inner umbrella, as might be expected, given the reduction in range and detection effects.

While these cases were specifically chosen for extensive and/or heavy precipitation, some differences between the radars and algorithms begin to appear when the only cases considered are those with precipitation indicated by at least one of the radars or the gauge network. This indicates estimation skill in "critical" cases. Rank correlation coefficients are smaller, relative to the full data sample (Fig. 8). Root-mean-squared errors (RMS errors) are of the order of the average observed rainfall value within this subsample of cases, namely 0.06 – 0.08 inch (Fig. 9). Horizontal smoothing of both the COMB and Z-R algorithm output reduces RMS error slightly (for example COMB 4KM vs. COMB in Fig. 9).

After further filtering of the data to include only cases where at least one sensor system indicated ≥ 0.1 inch of rain, some more inter-algorithm differences are indicated. As shown in Figs. 10-11, while the DPA algorithm (from KTLX) appears to have a higher correlation with gauge values than do the COMB and Z-R (from KOUN), the RMS error of the DPA is slightly higher (Fig. 11). This condition holds for both the entire umbrella and the inner portion. It is probably an indication of nonlinearity in the radar-gauge relationship, as shown in the next section. Similar results were obtained when the data were filtered still further to include only cases with 0.2 inch of rain observed; this sample contained < 500 cases and results should be confirmed with a larger one.

The installation of the KOUN unit within 20 km of the KTLX unit does present a rare opportunity to investigate the statistical interaction between observations from two functionally similar radars that view storm events from similar ranges and angles. We found that rainfall estimates from the two radars were more closely correlated with each other than with the gauge observations, as might be expected (Fig. 12). On the other hand, while the KOUN-KTLX correlation is high, (> 0.85) this indicates that there are still appreciable differences between their estimates, beyond long-term bias.

A few trials indicate that a weighted average of the estimates from both radars produce a product with more skill than is shown by estimates from either radar considered alone. Such a statistical combination of radar observations might prove useful even with radars of different operating characteristics, given that they are sited fairly close together (e.g. Terminal Doppler or ASR aviation radars). We will further examine this possibility when more KOUN data become available, and with combinations of WSR-88D and Terminal Doppler Weather Radar data.

Effects of spatial filtering of rainfall estimates

As noted above, it appears that some component of the Combined algorithm introduces spatial discontinuities into the rainfall fields. A simple noise-reduction filtering algorithm was applied to determine the magnitude of the noise effects and to see if information in the longer-wavelength features might be partially recovered. This filter is a nine-point local consensus average, applied to all 2-km grid bins with precipitation or with precipitation in all of the surrounding bins. The consensus average is the mean of the surrounding values excluding the two highest and lowest values. Outliers and some zero-precipitation bins surrounded by nonzero bins should logically be corrected by this filter, as shown in Fig. 13a,b.

The filtering also has an effect in reducing systematic overestimation errors for larger radar amounts. For a set of 920 cases in which either gauge or radar indicated measurable precipitation, radar overestimation is evident for most values above 0.1 inch h^{-1} (Fig. 14). However the estimation is most pronounced for the Z-R algorithm (plotted open triangles) and the original Combined-algorithm output (plotted blue diamonds). Each plotted point represents the mean radar and gauge values of approximately 100 pairs. A similar result was obtained when a collocated set of KOUN and KTLX DPA estimates were examined (Fig. 15).

Spatial filtering also has an effect in reducing RMS errors, as shown in Figs. 16-17. Overall RMS errors are of the same magnitude as the rainfall itself (0.14 inch for the sample in Fig. 16, 0.15 inch for the sample in Fig. 17). The consensus-average filter reduced the magnitude of the Combined algorithm RMS error by about 20%. Filtering had less effect on the Z-R algorithm output.

Initial Conclusions

Overall, the performance of the Combined algorithm is roughly comparable to that of the Z-R algorithm and, for areas with heavier precipitation, better than that of the Z-R algorithm or the operational KTLX rainfall estimates. The output of the existing Combined algorithm features some high-frequency noise that appears as isolated bins with anomalous high or low values relative to their neighbors. The source scientists are still engaged in refining the Combined algorithm and preprocessing for the dual-polarization moments, particularly Kdp (Ryzhkov, personal communication). We found that spatial filtering of one-hour estimates substantially improved some verification statistics such as RMS error relative to rain gauges.

The Combined algorithm appears to deliver more improvement over Z-R within 120 km of the radar site. This might be expected since the dual-polarization technique has been developed with the aim of improving rainfall estimates in situations with unusual raindrop size distributions or hail effects, rather than estimating near-surface precipitation rates in atmospheric columns where the radar detects only mixed-phase precipitation or snow aloft. Bright-band enhancement can still appear in the Combined algorithm estimates (for example the November and February cases, Figs. 4 and 5). A range-correction component might be necessary to compensate for reflectivity profile artifacts in these radar estimates.

One shortcoming of the Combined algorithm at this stage is a significant level of noise in the 1-hour estimates. This is a potential visual distraction, and our results indicate that even simple spatial filtering leads to improvements in radar-gauge correlations. Implementation of full connectivity between the Hydrometeor Classification Algorithm (HCA) and precipitation algorithms, and real-time detection of nonuniform-beam-filling situtations in the Kdp calculation, should mitigate the noise conditions by treating the root causes.

In the two situations shown here, it appears the Combined algorithm did little to mitigate bright-band enhancement of precipitation. Plans for the next version of the algorithm call for implementation of an adjusted Z-R relationship for those zones where the radar detects melting snow (Ryzhkov 2006). However, it is likely that some form of range correction must ultimately be applied to make the best possible estimate of surface precipitation in areas where the lowest radar beam detects a hydrometeor distribution different from that near the surface.

While the KOUN precipitation estimates were not more accurate than those from the operational KTLX unit, this might be due to the relative operating status of the two units. However, we should insure that the KOUN unit and its algorithms at least match the performance of nearby WSR-88D units prior to operational fielding of the dual-polarization electronics and algorithm packages.

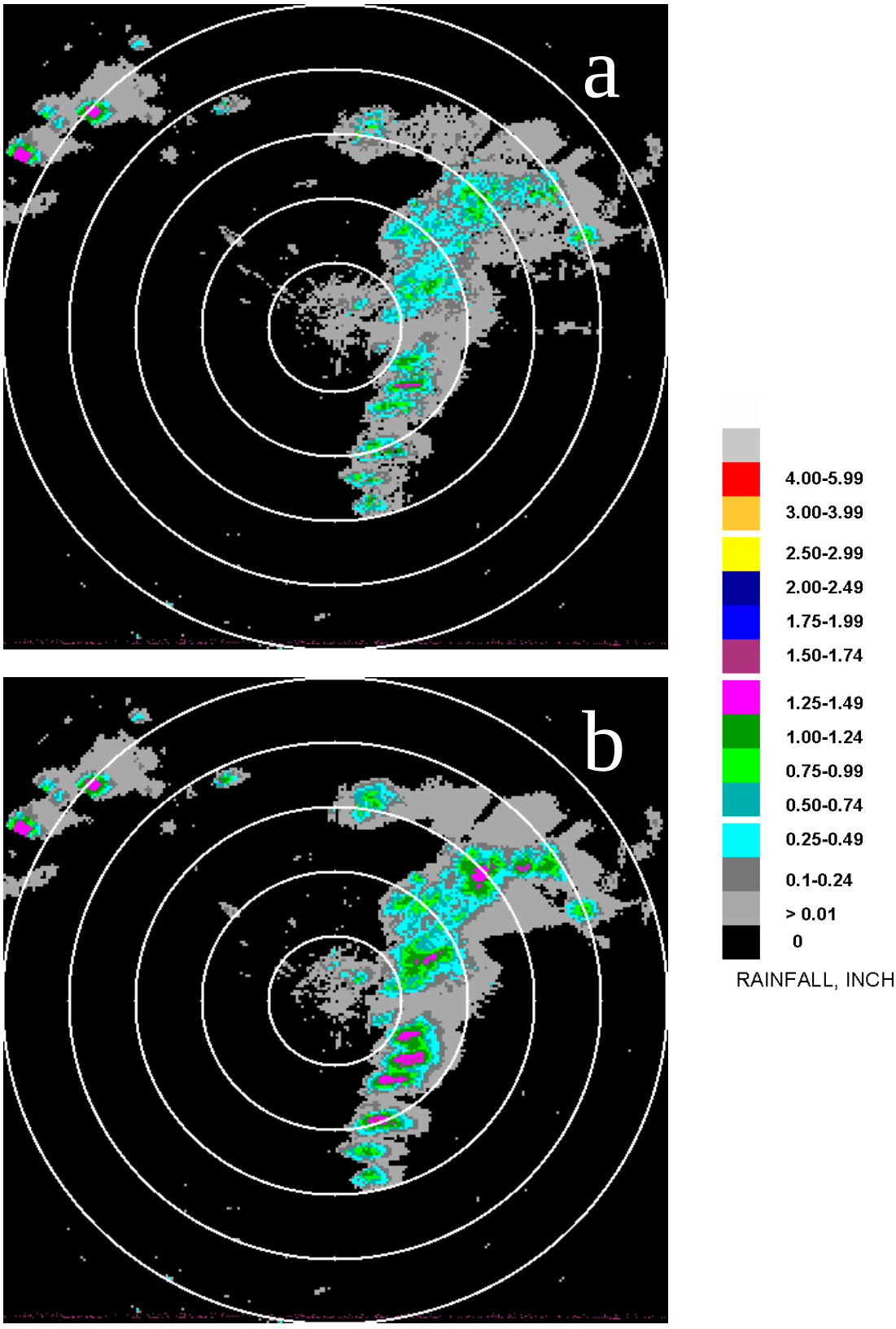

Figure 1. One-hour precipitation within the KOUN umbrella, valid 0000 UTC 22 April 2004. Images are from (a) dual-polarization "Combined" algorithm and (b) Z-R horizontal polarization Relationship.

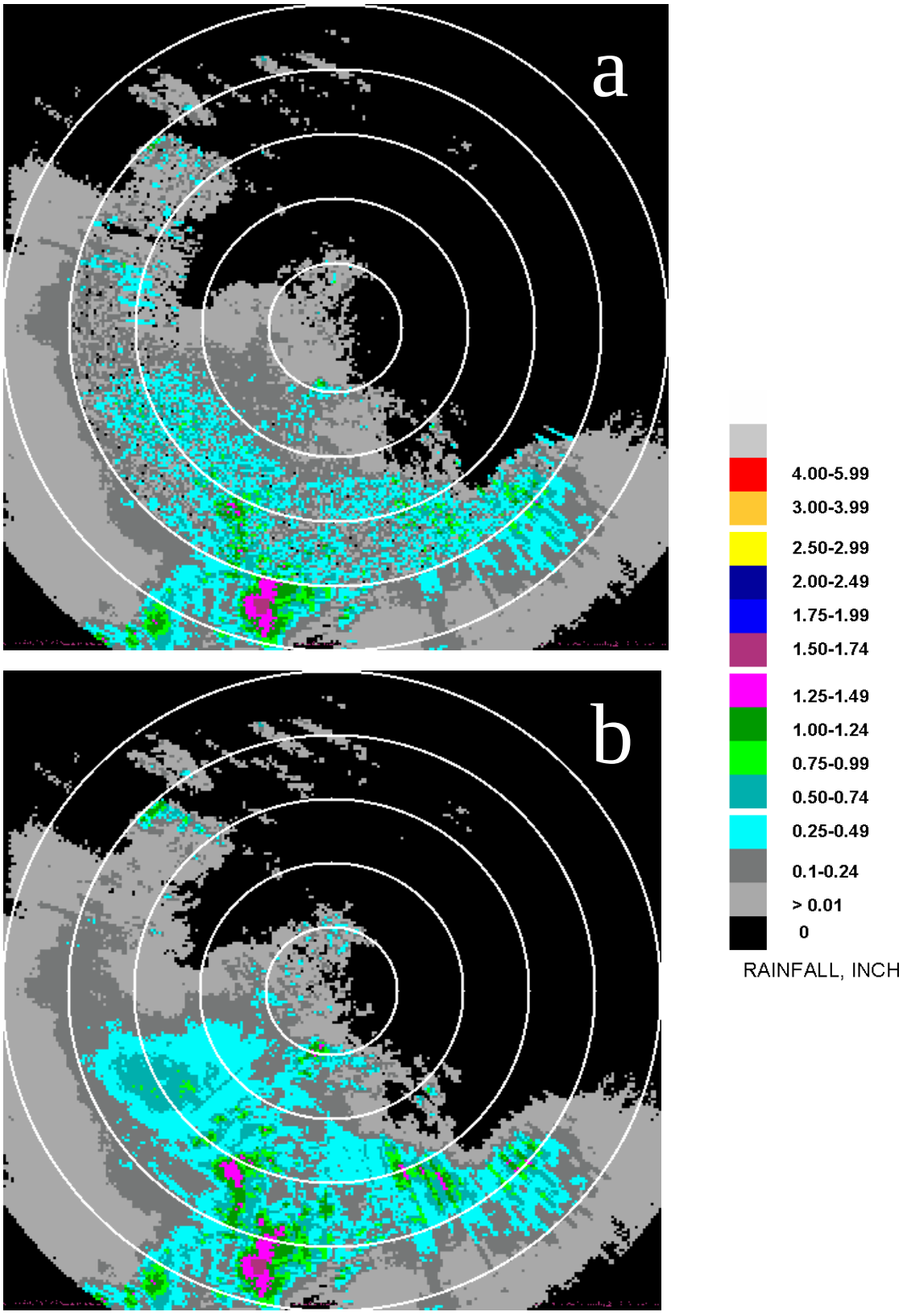

Figure 2. As in Fig. 1 except for 0300 UTC, 3 June 2004.

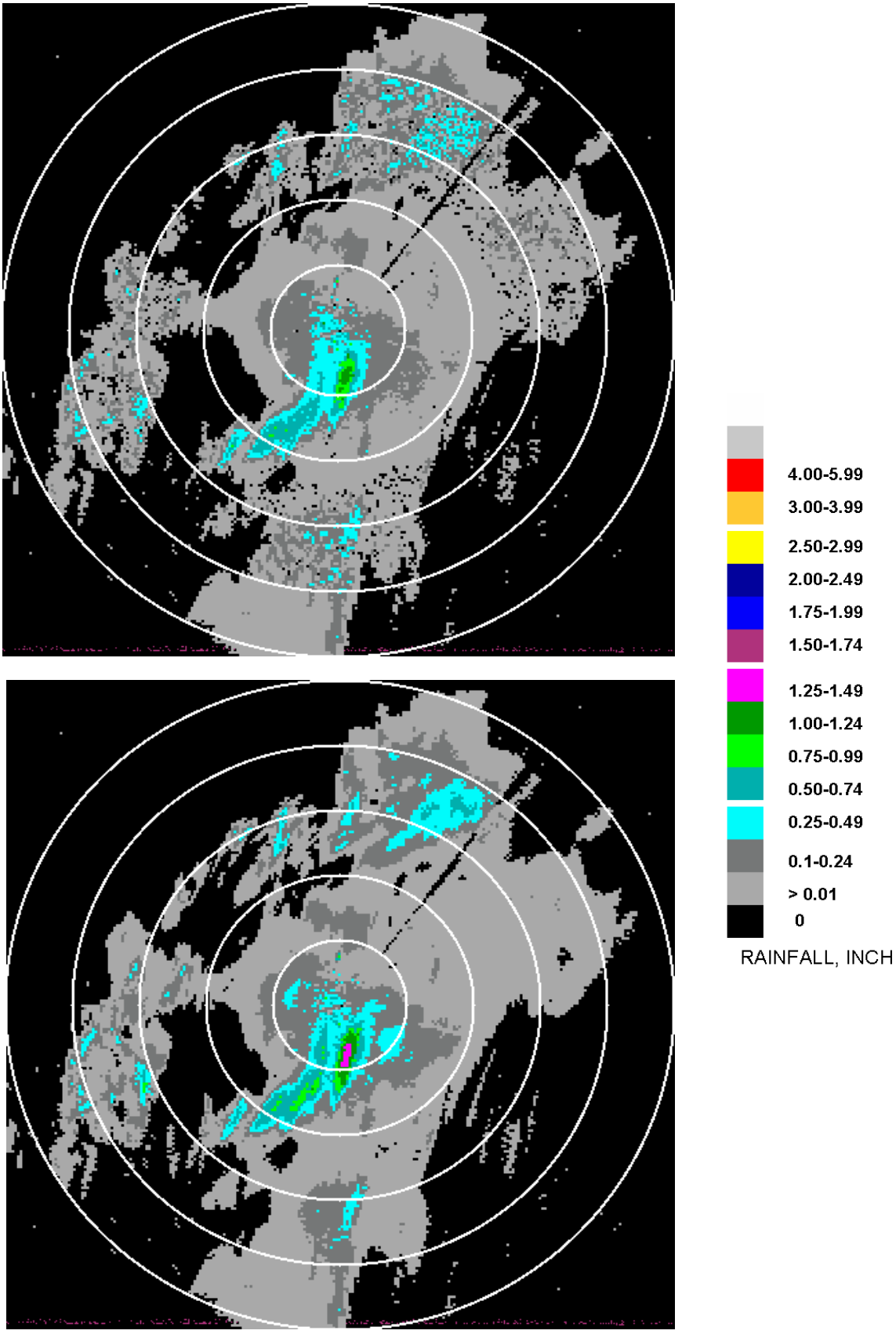

Figure 3. As in Fig. 1 except for 1600 UTC, 9 June 2004.

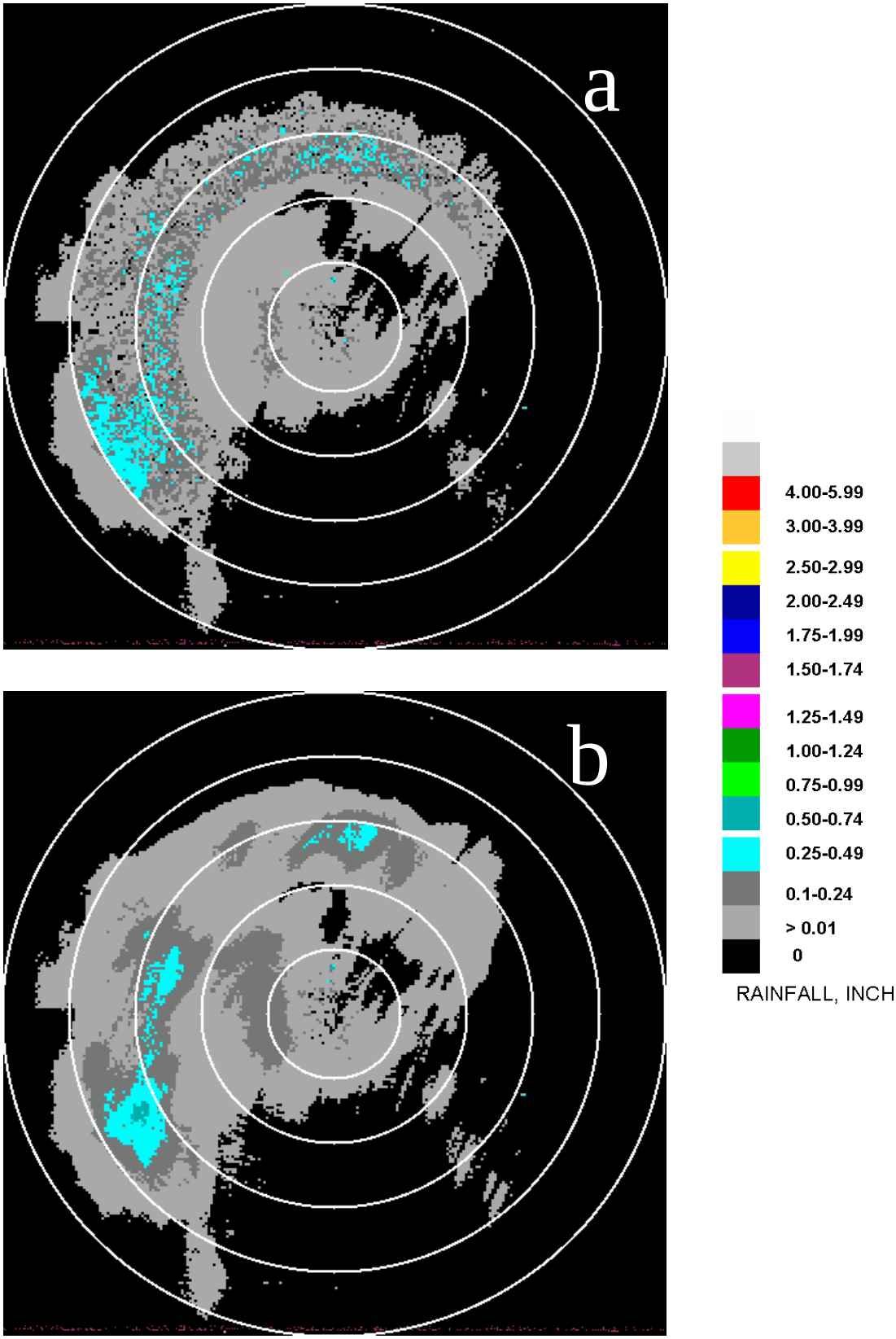

Figure 4. As in Fig. 1 except for 1200 UTC, 15 November 2004.

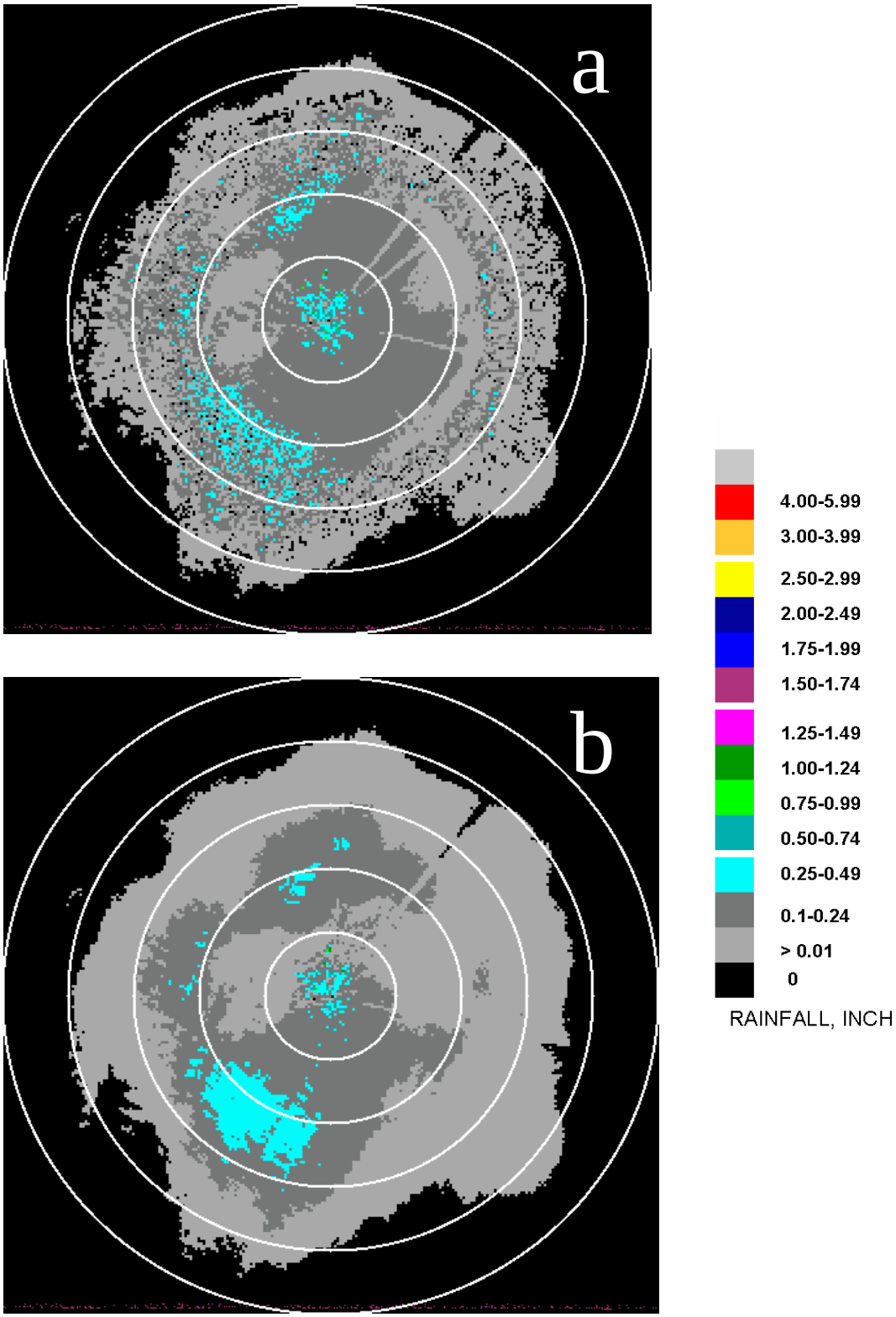

Figure 5. As in Fig. 1 except for 0900 UTC, 6 February 2005.

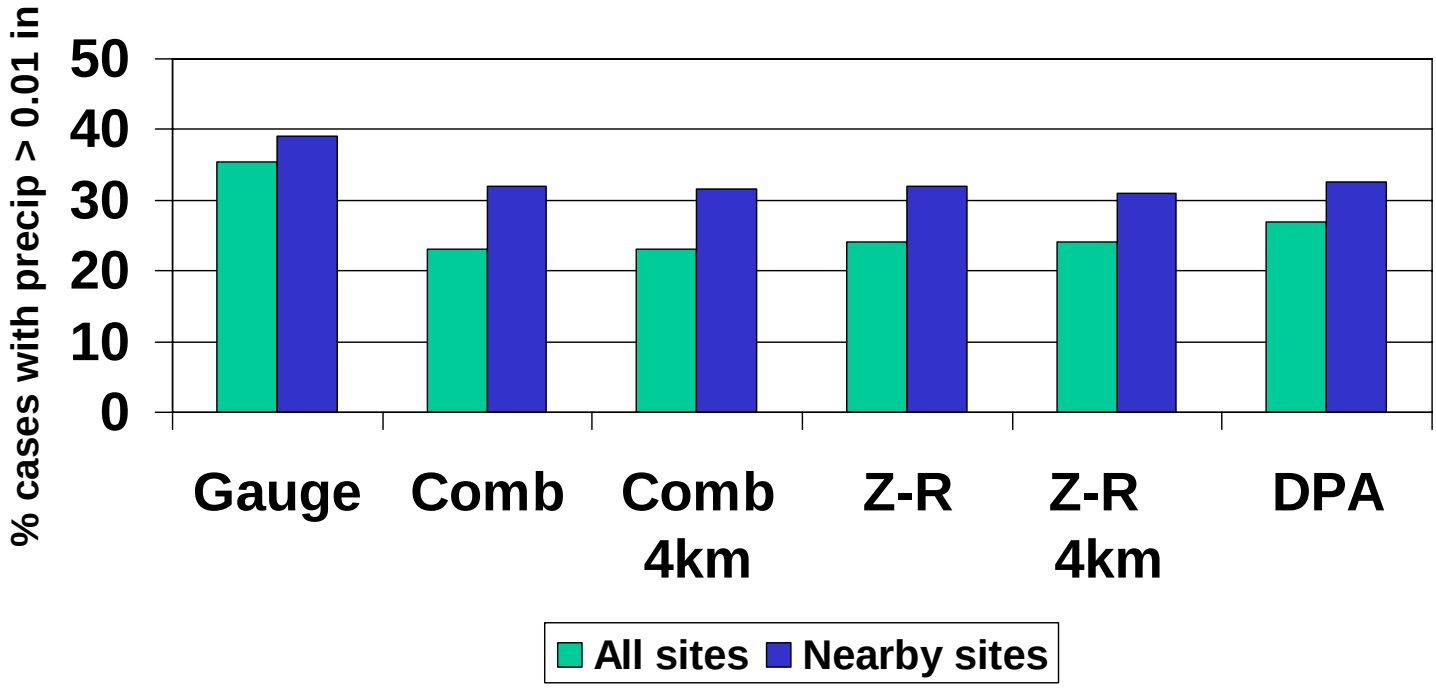

Figure 6. Percent of radar-gauge pairs with > 0.01 inch rainfall in one hour. Green bars are for all gauge sites (4787 cases), blue bars are for sites within 120 km of the KOUN unit (1901 cases).

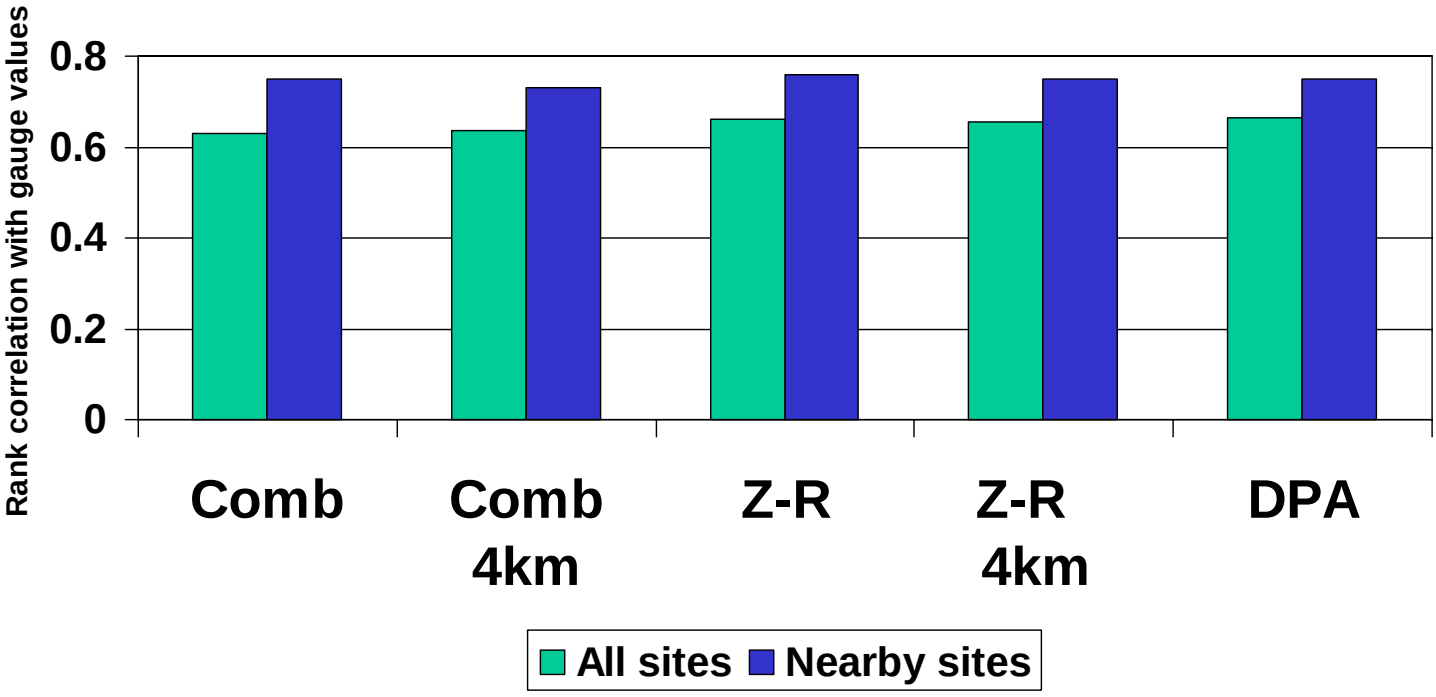

Figure7. Rank correlation between radar estimates and gauge values, for all 4787 cases (green bars) and for gauge sites within 120 km of KOUN (1901 cases).

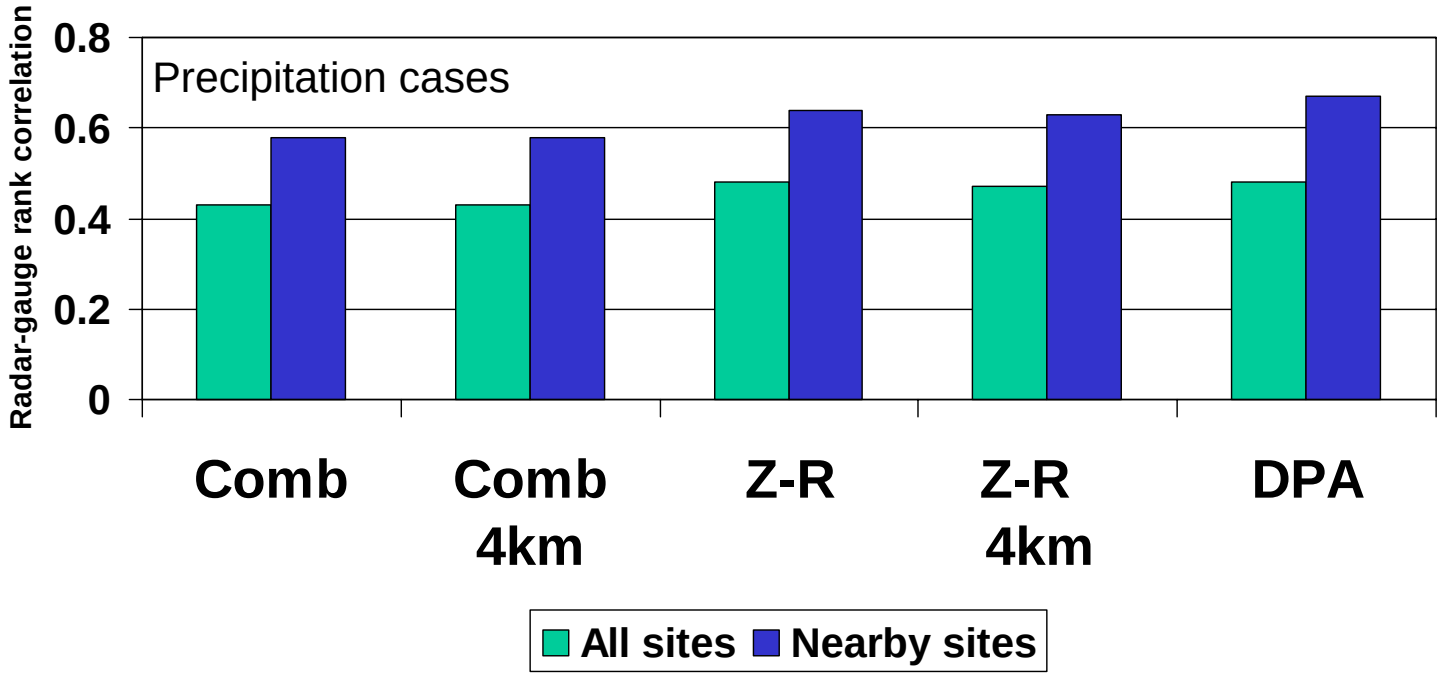

Figure 8. Rank correlation coefficient between radar and gauge reports for all 4075 cases in which at least one sensor indicated measurable precipitation (green bars) and for 1901 precipitation cases within 120 km of KOUN (blue bars).

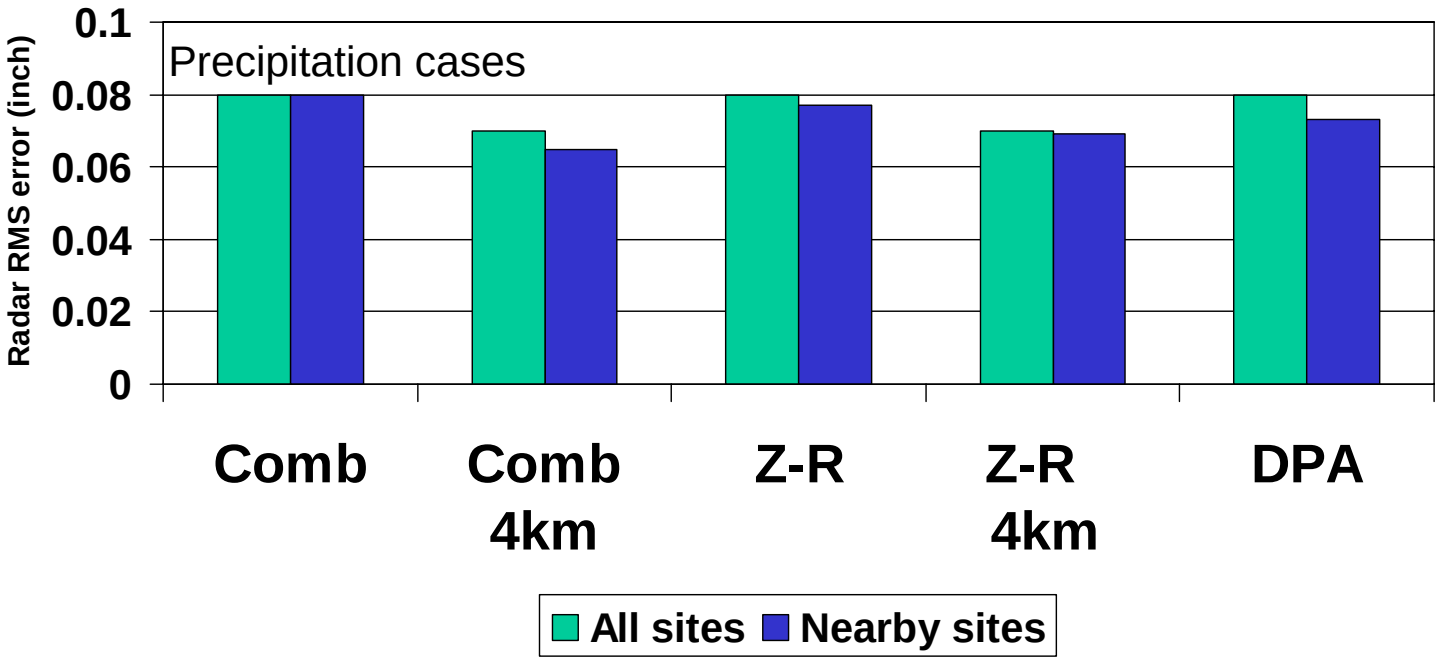

Figure 9. RMS error of radar estimates relative to gauge values, for cases in which at least one sensor indicated measurable precipitation. Range stratification is as in Fig. 8

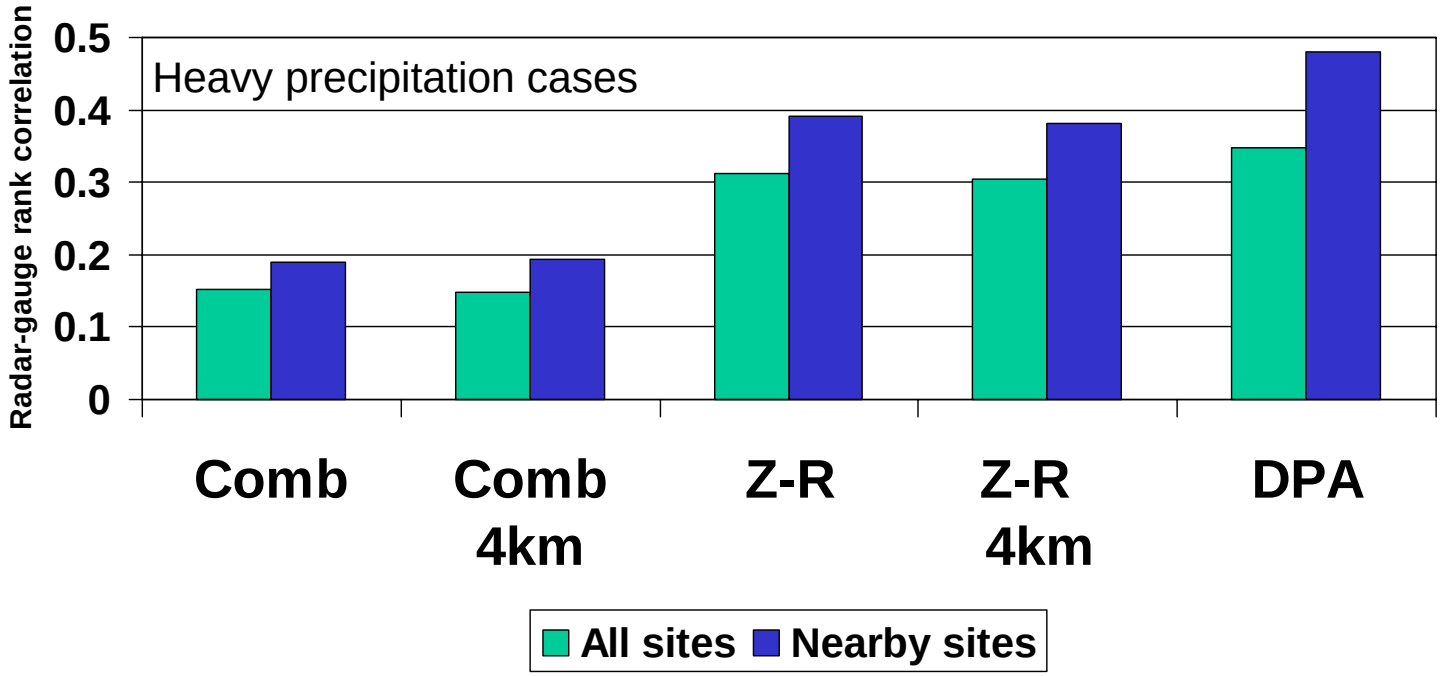

Figure 10. As in Fig. 8, except for 1006 cases with at least one sensor indicating > 0.1 inch rainfall (green bars), and for 553 such cases within 120 km of the KOUN site.

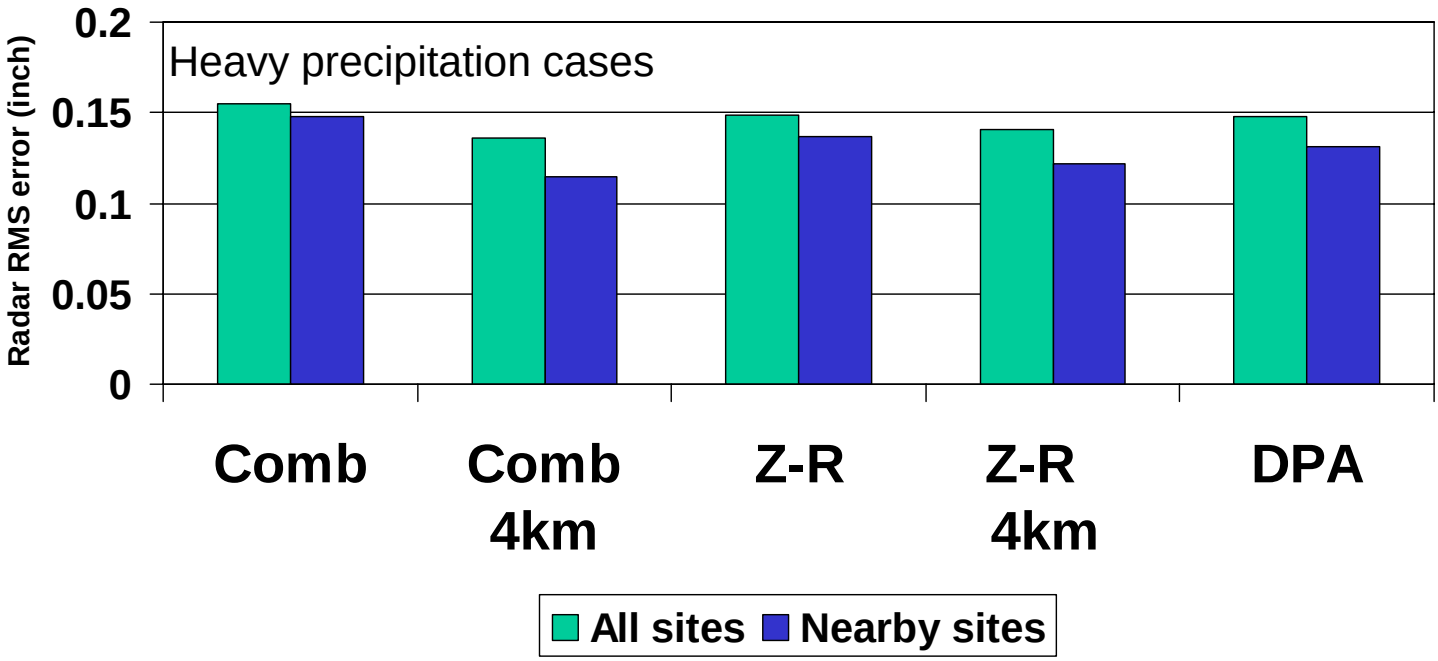

Figure 11. As in Fig. 9, except for 1006 cases with at least one sensor indicating > 0.1 inch rainfall. Range stratification as in Fig. 12.

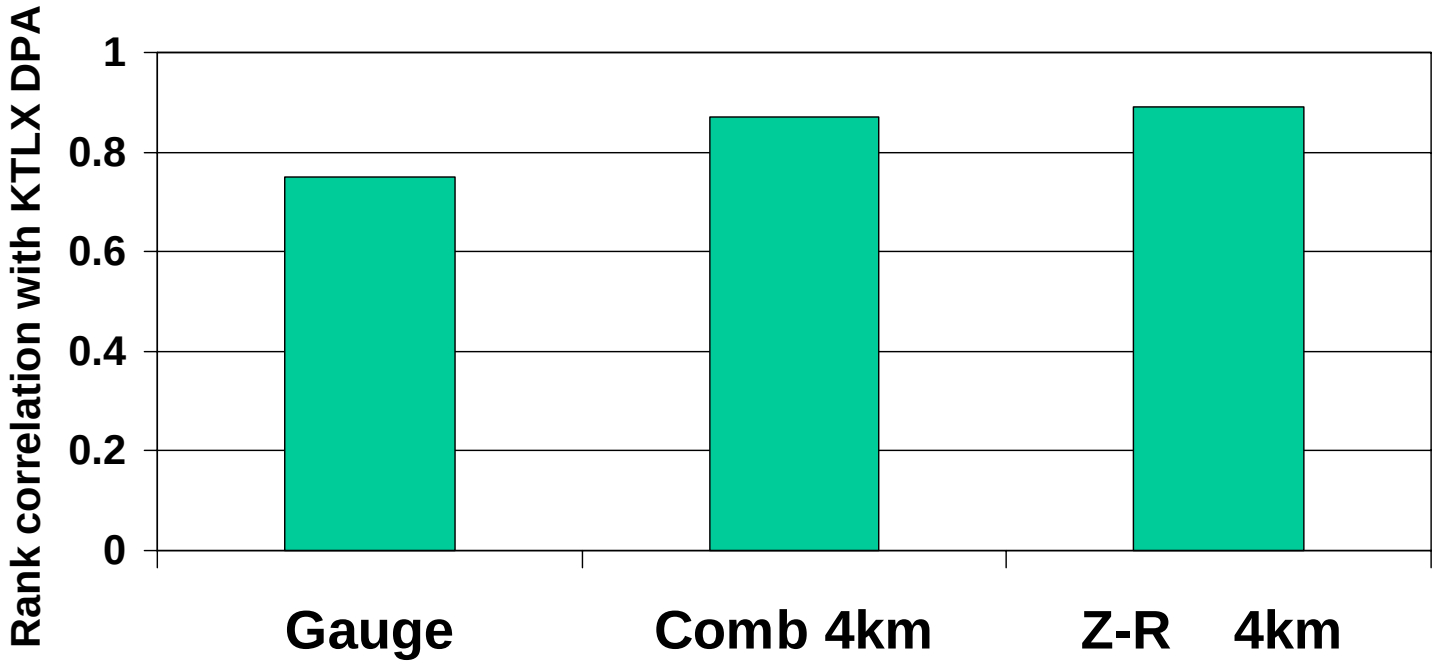

Figure 12. Rank correlations of precipitation estimates relative to those of the KTLX WSR-88D unit, for all 4787 radar-gauge pairs.

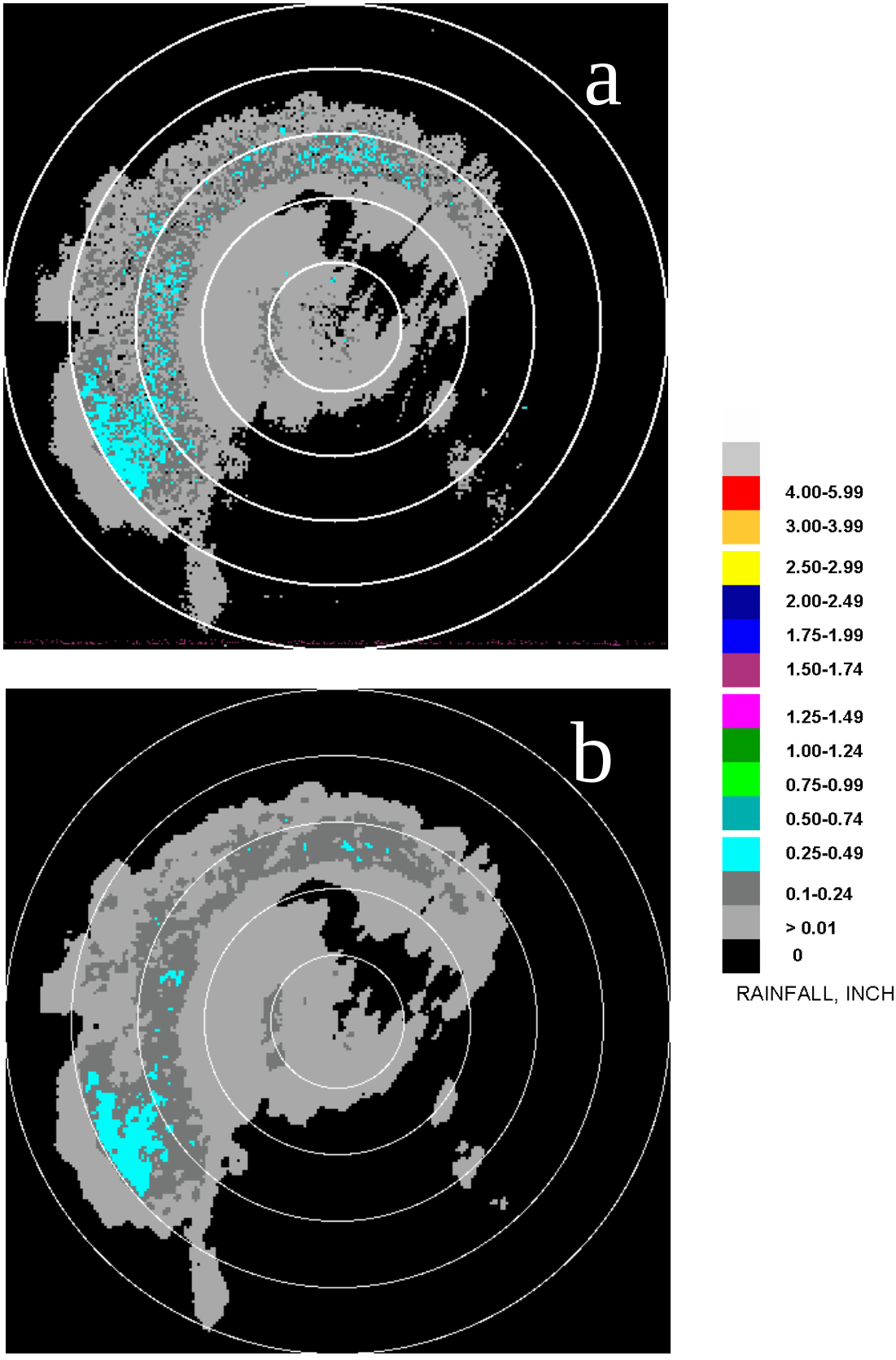

Figure 13. One-hour precipitation within the KOUN umbrella, valid 0000 UTC 22 April 2004. Images are from (a) dual-polarization "Combined" algorithm and (b) Combined algorithm after local consensus averaging.

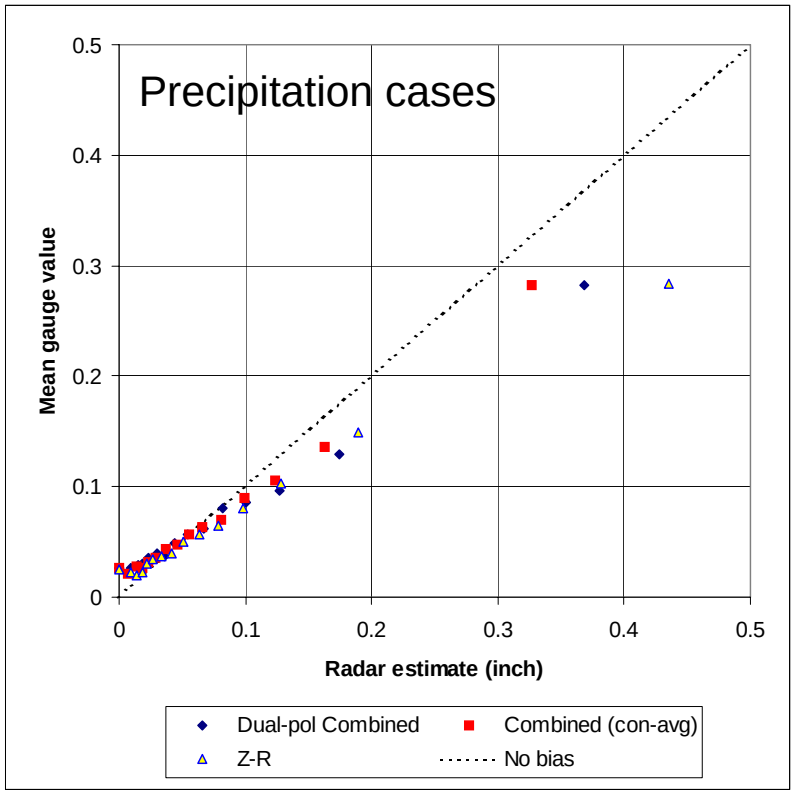

Figure 14. Expected rain gauge values for a range of radar estimates. Each plotted point represents ~100 individual cases. All cases feature nonzero precipitation as indicated by at least one sensor system.

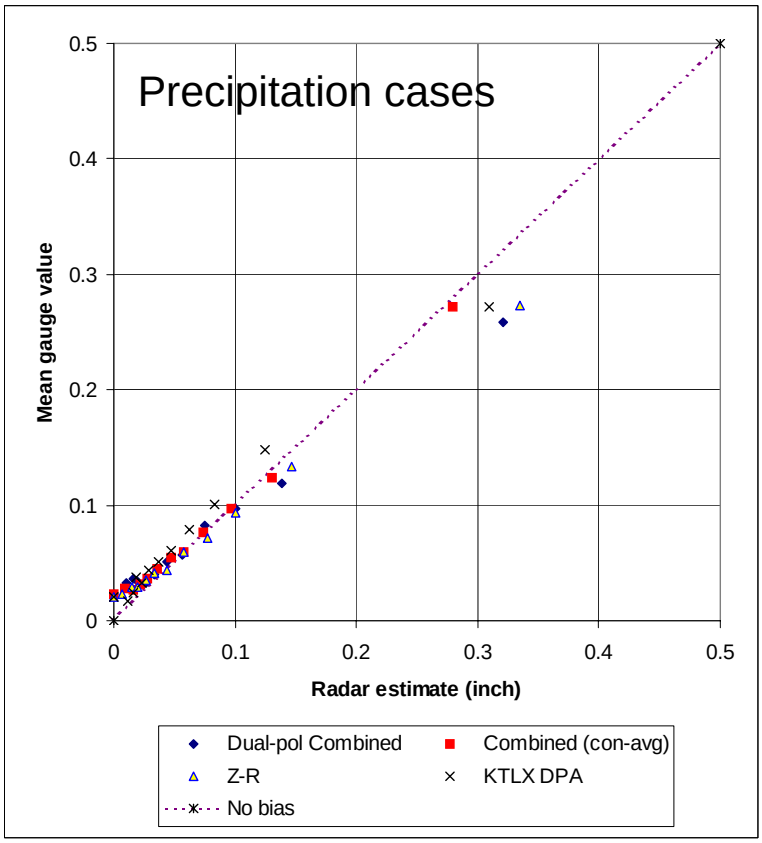

Figure 15. As in Fig. 14, except for a smaller sample including WSR-88D DPA estimates from the KTLX site.

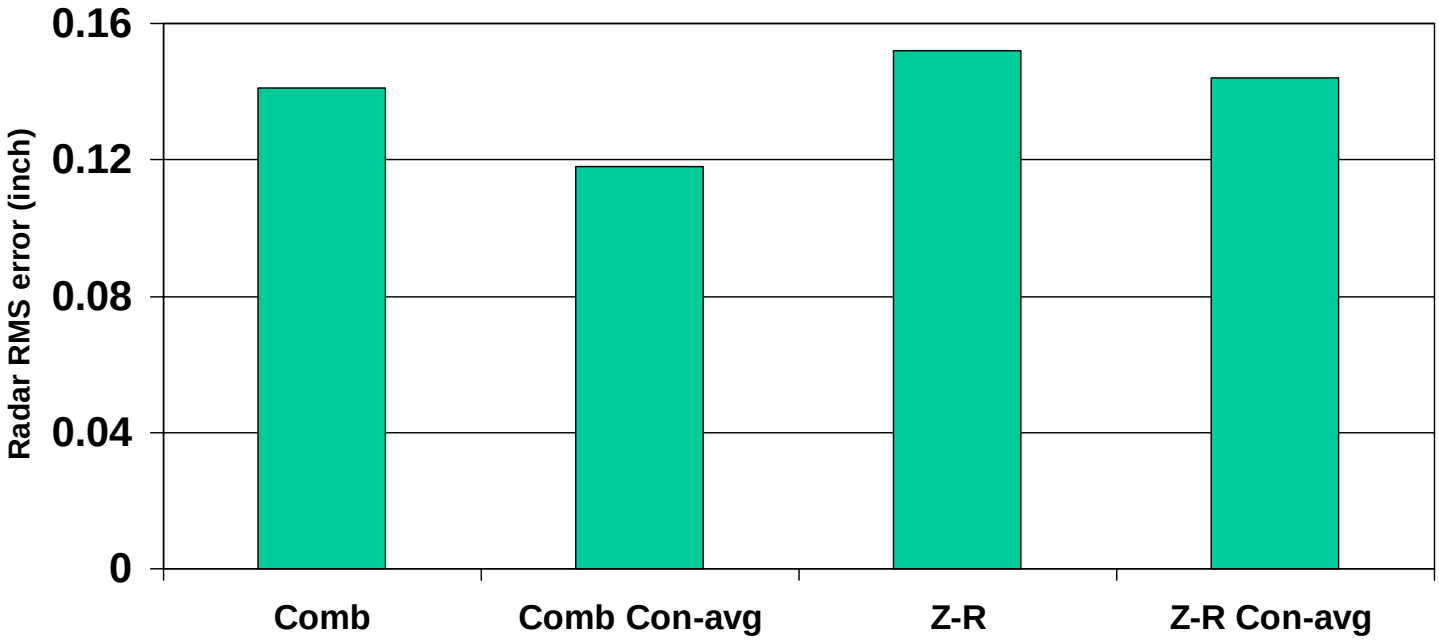

Figure 16. RMS errors for Combined and Z-R rainfall algorithms, KOUN data. Analysis of 926 cases with 0.1 inch of precipitation observed by either radar or gauge. Con-avg refers to consensus average.

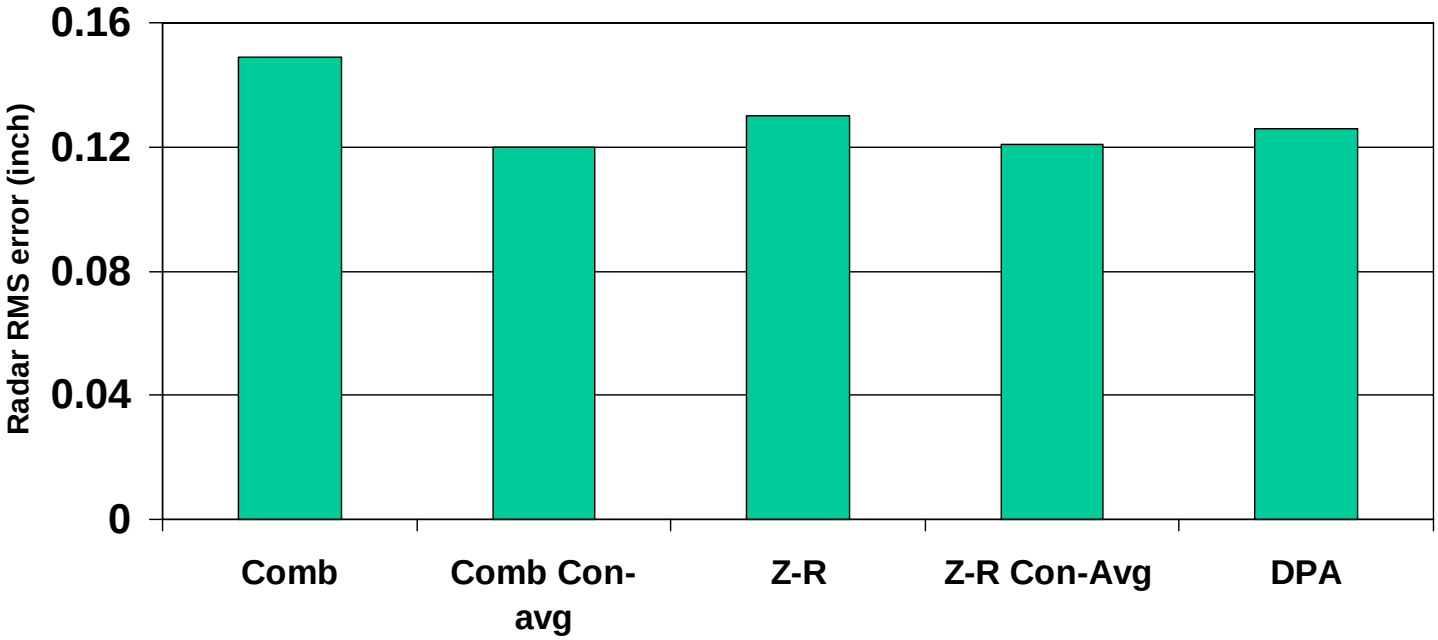

Figure 17. As in Fig. 16, except for 430 cases including collocated estimates from KTLX (DPA product).

II. Comparative Analysis of Hydrometeor Classification Algorithm (HCA) and WSR-88D Radar Echo Classifier (REC)

We've undertaken an analysis of the NSSL dual-polarization Hydrometeor Classification Algorithm (HCA) to determine if its output might be applied to horizontal-polarization precipitation estimates as are currently operational within the WSR-88D system.

Much effort has been devoted to identifying and removing nonprecipitation (NP) echoes from radar reflectivity data prior to its interpretation for precipitation accumulation. In the WSR-88D system, the NCAR-designed Radar Echo Classifier (REC) has been designed primarily to remove ground targets (clutter and anomalous propagation) from reflectivity that enters the Digital Hybrid array (DHR) product, which in turn enters the Precipitation Processing System (PPS). Ongoing work at NCAR is dedicated to improving clutter detection and adding a general precipitation detection feature. The HCA developed by NSSL is designed to identify both ground and aerial targets, and to differentiate among hydrometeor types and other aerial targets such as migrating birds and insects.

While clutter and AP still cause some serious errors in WSR-88D precipitation accumulations, light accumulations from birds and insects are more spatially and temporally prevalent, particularly during the spring and autumn migration seasons. Return from birds can reach 30 dBZ for brief periods depending on the density of birds and radio propagation conditions. The present REC was not designed to identify biota, which produce an echo spectrum closely resembling light precipitation. Light accumulations of a few hundredths of an inch are rather common in precipitation products, and these must be removed by human analysts before the data entire hydrologic applications.

Subjective interpretation of reflectivity data with and without filtration by HCA output suggests that the HCA is much more effective at identifying biota than is the REC. Two sets of image pairs in Figs. 18-19 are typical of results when the KOUN dual-polarization unit and the KTLX WSR-88D see similar combinations of biota and precipitation. In these images reflectivity has been mapped to a 1-km local Cartesian grid with coverage of about 230 km radius. The images are from about 0700 UTC, 13 May 2005, when a mesoscale convective system was approaching the Oklahoma City area from the northwest. Return from migrating birds was evident near the radar sites to the south, east, and north (Figs 18a, 19a). In the area of biota returns, the KOUN unit indicated reflectivities as high as 24 dBZ, in light green, and KTLX, reflectivities as high as 19 dBZ (dark blue).

Following filtration by HCA, much of the biota returns are eliminated , as shown in Fig. 18b. Here, all reflectivity values identified as nonprecipitation were reset to below the 5-dBZ display threshold. Some vestiges of the biota pattern remain, but most of the targets were clearly identified. Filtration by the REC did not eliminate the biota, as shown in Fig. 19b.

To better assess the potential impact of the HCA on precipitation estimates, we compared the results of the HCA filtration with a subjective manual editing of the 16-level reflectivity images. An OHD staffer with experience in radar interpretation manually converted the contents of a PPM image file such that echoes judged to be nonprecipitation were converted to the black

below-threshold color category, much as the HCA filtration does. Results of manual editing of Fig. 19a appear in Fig. 20. Both the HCA- and manually-filtered images were then quantitatively compared with the original unfiltered one. For each pixel, representing a 1-km-square region, if the original image had an echo ≥ 5 dBZ, the two editing results were compared. If they agreed (both retained or both rejected the echo), the HCA was considered to be "correct." The percentage correct was determined for the entire reflectivity image in this manner. In the case shown in Fig. 1, approximately 92% of the HCA editing decisions were confirmed by the manual check

A similar comparison was made between manually-edited KTLX base reflectivity and reflectivity filtered by REC. In the case shown in Figs. 19-20, about 77% of the REC editing decisions were confirmed by the manual check.

Though radar sensitivity, radio propagation, and geometry factors rendered most KOUN/KTLX image pairs slightly different, we found that in general the two radars indicated precipitation and nonprecipitation echoes in roughly the same areas at the same times.

A comparison of several sets of image pairs indicated that as the percentage of the reflectivity area covered by precipitation increased, the more closely the REC and HCA filtering output agreed with the manual filtering and with each other. This result could be expected because the cases were selected to show the effects of automated filtering when the PPI is dominated by a mixture of precipitation and biota, and because HCA specifically identifies biota while REC does not. Results are summarized in Fig. 21, in which percentage of editing decisions in which HCA and REC agreed with manual results are displayed as functions of the percentage of all reflectivity points retained after subjective manual editing. The percentage agreement is generally between 85% and 90% for HCA regardless of the degree to which the images were dominated by biota. For REC, agreement is below 50% when more than half of the reflectivity area was judged to be biota. Overall, the HCA had consistently higher agreement with the manual process than did REC.

While the results shown thus far were based on the work of only one or two analysts, we believe that they are representative of those that would be produced by several analysts working independently. To test this assumption, we had two more analysts (a total of 4) repeat the analysis. Three attempted to edit at least 6 of the 9 image sets; the fourth edited two. Agreement between manual and automatic editing for all the analysts are shown in Fig. 22. With the exception of one or two cases (such as 0700 UTC on 16 May 2005) the analysts generally agreed on their assessment of the HCA and REC.

It appears that a final check to remove isolated reflectivity points could improve either HCA or REC, since near the radar the HCA generally leaves a scattering of nominal precipitation points (see Fig. 18b).

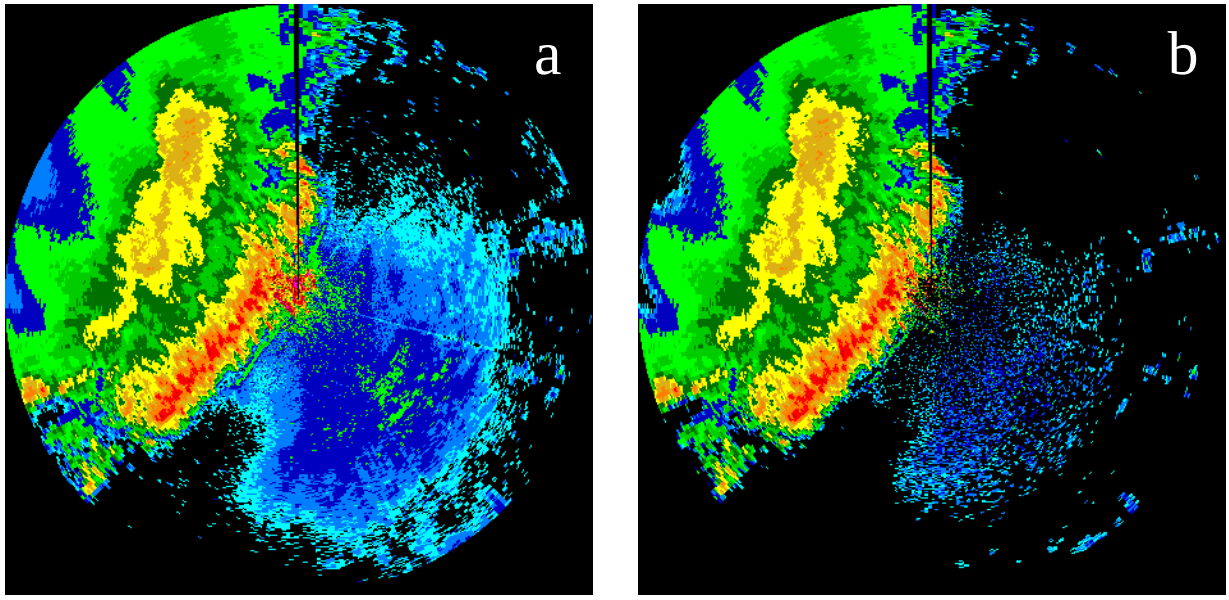

Figure 18. Reflectivity at 0.5° elevation angle from Norman OK dual-polarization radar KOUN, Image in (a) is original reflectivity, (b) after filtration for nonprecipitation echoes by HCA.

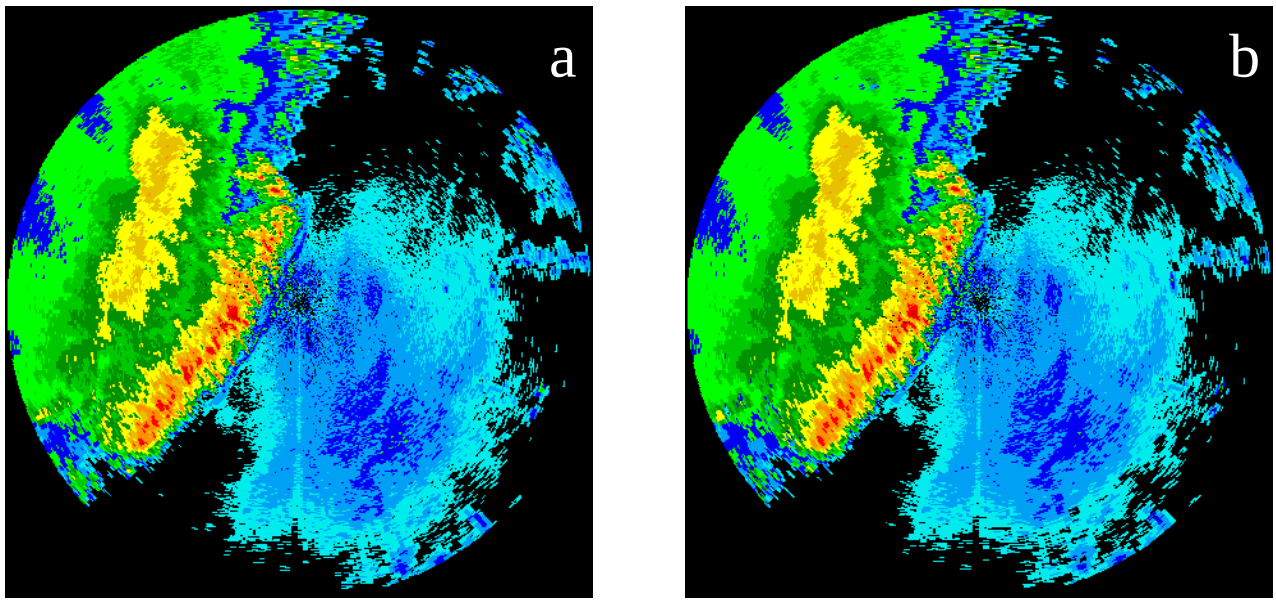

Figure 19. Reflectivity at 0.5° elevation angle from WSR-88D KTLX (Twin Lakes OK), Image in (a) is original reflectivity, (b)digital hybrid scan after filtration by REC.

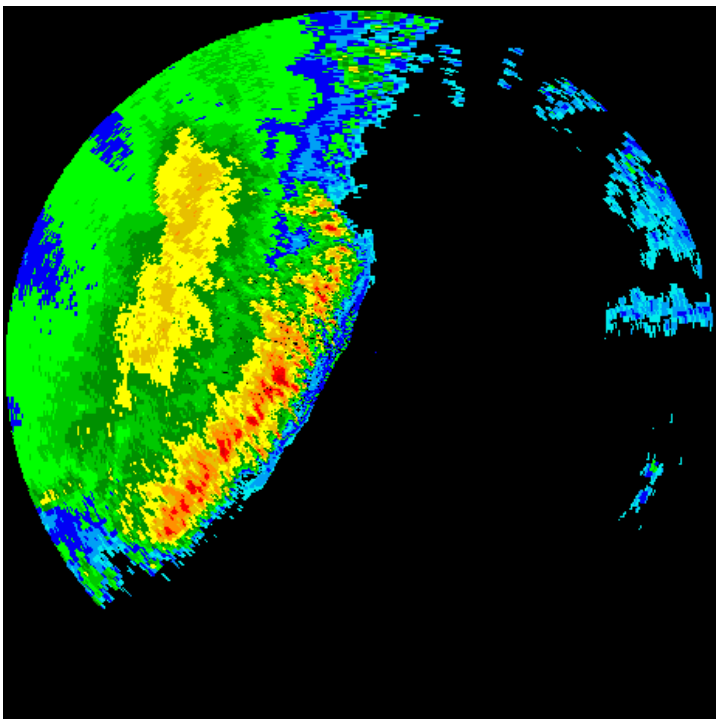

Figure 20. Reflectivity field from Fig. 2a after manual editing to remove nonprecipitation echoes.

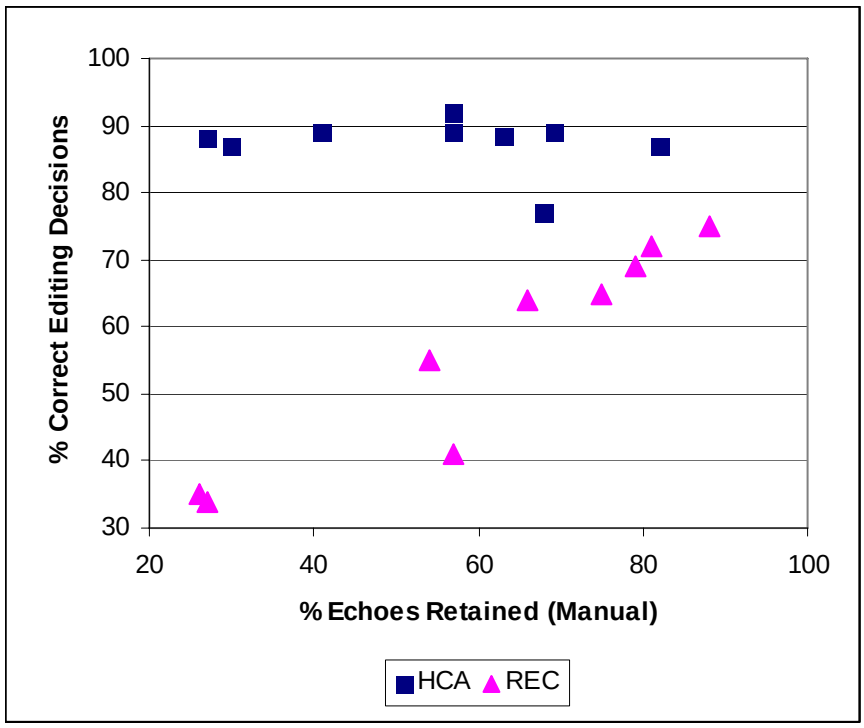

Figure 21. Percentage of echo editing decisions by Hydrometeor Classifier Algorithm (HCA) and Radar Echo Classifier (REC) judged correct, based on manual interpretation of the imagery. Both algorithms yield > 70% correct decisions in images dominated by precipitation; HCA performs better than REC when the image is dominated by biological targets or other nonprecipitation echoes. The focus in this set of cases was images with a mixture of precipitation and biological targets, though anomalous propagation was evident in some HCA cases.

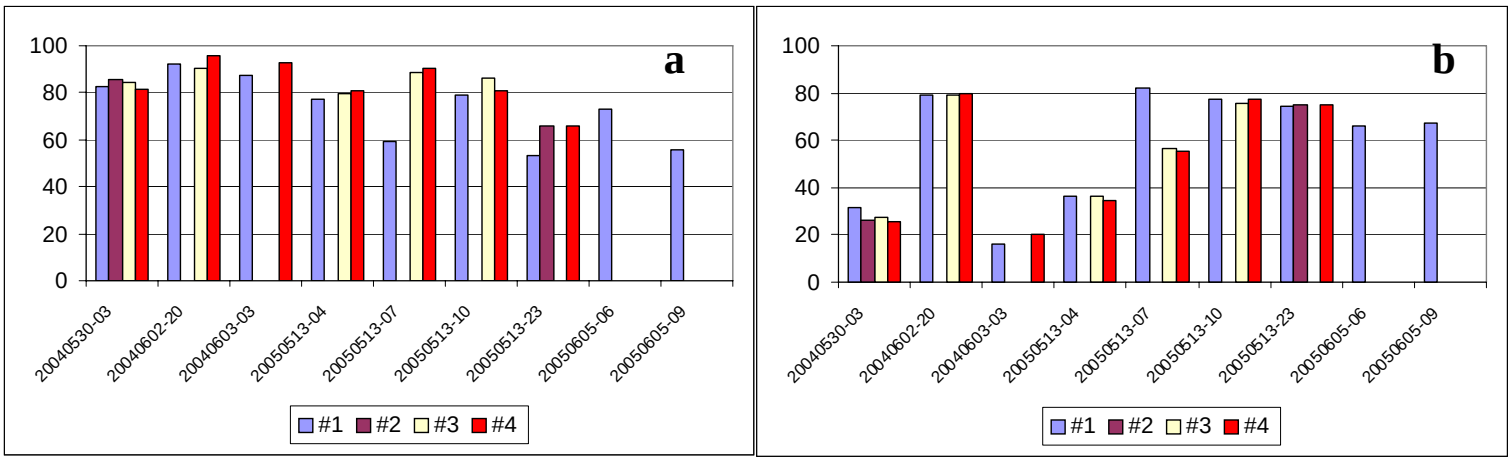

Figure 22. Degree of agreement between manual and automated editing decisions for four analysts. Results are for (a) HCA applied to KOUN data and (b) REC-EPRE applied to KTLX data.

III. Analysis of NSSL Precipitation Algorithms Applied to NCAR S-pol Dual-Polarization Radar Data

In an effort to validate the applicability of the NSSL dual-polarization precipitation algorithms outside the Oklahoma area, we have initiated a study in which the algorithms are applied to historic data collected over east-central Florida in 1998, by the NCAR S-pol radar unit. These data were collected during the PRECIP98 (or TEFLUN-B) experiment (NCAR 1999).

As a research radar, the S-pol unit was often operated in modes dissimilar to operational WSR-88D volumetric scanning. Moreover, some of its functional characteristics such as range gate spacing differ from those of the WSR-88D. Considerable effort was invested in locating suitable events in terms of rainfall and radar observation coverage, as well as spatially interpolating the S-pol moments to a resolution of 1º azimuth by 1000 m range spacing.

We have successfully decoded and remapped the basic dual-polarization moments, and derived rainfall estimates by applying the convective Z-R relationship $Z = 300R^{1.4}$ and the NSSL "Synthetic" algorithm (Ryzhkov et al. 2005). The estimates are derived from moments at the lowest antenna elevation angle, generally 0.5º. Note that we have not attempted to apply quality control beyond filtering out backscatterers with a cross-correlation < 0.90 (following the current NSSL convention) or returned power of < -112 dB (on the suggestion of NCAR staff).

The data initially supplied by NCAR proved to have excessive noise in the φ_{DP} and Kdp moments, which resulted in very noisy rainfall fields. After consultations with NCAR staff we were supplied with new data, treated with improved preprocessing, which has proved to have statistical characteristics similar to those of observations from the KOUN radar.

Examples are shown in Figs. 23-24, which depict 1-hour precipitation during two events in September 1998. Note that there is no filtering for general system noise or ground clutter, and that the lowest nonzero rainfall threshold is lower than that of WSR-88D products, hence the rainfall coverage appears exceptionally large. Initial results indicate that the algorithm output is realistic, but that it still contains noise due to nonmeteorological spatial variations in the Kdp field.

When the latest NSSL algorithms have been finalized, we will investigate Florida-area estimates to determine if the level of agreement between NCAR S-pol and KMLB is similar to the correlation between KOUN and KTLX, in terms of areal coverage of measurable precipitation and precipitation exceeding various thresholds.

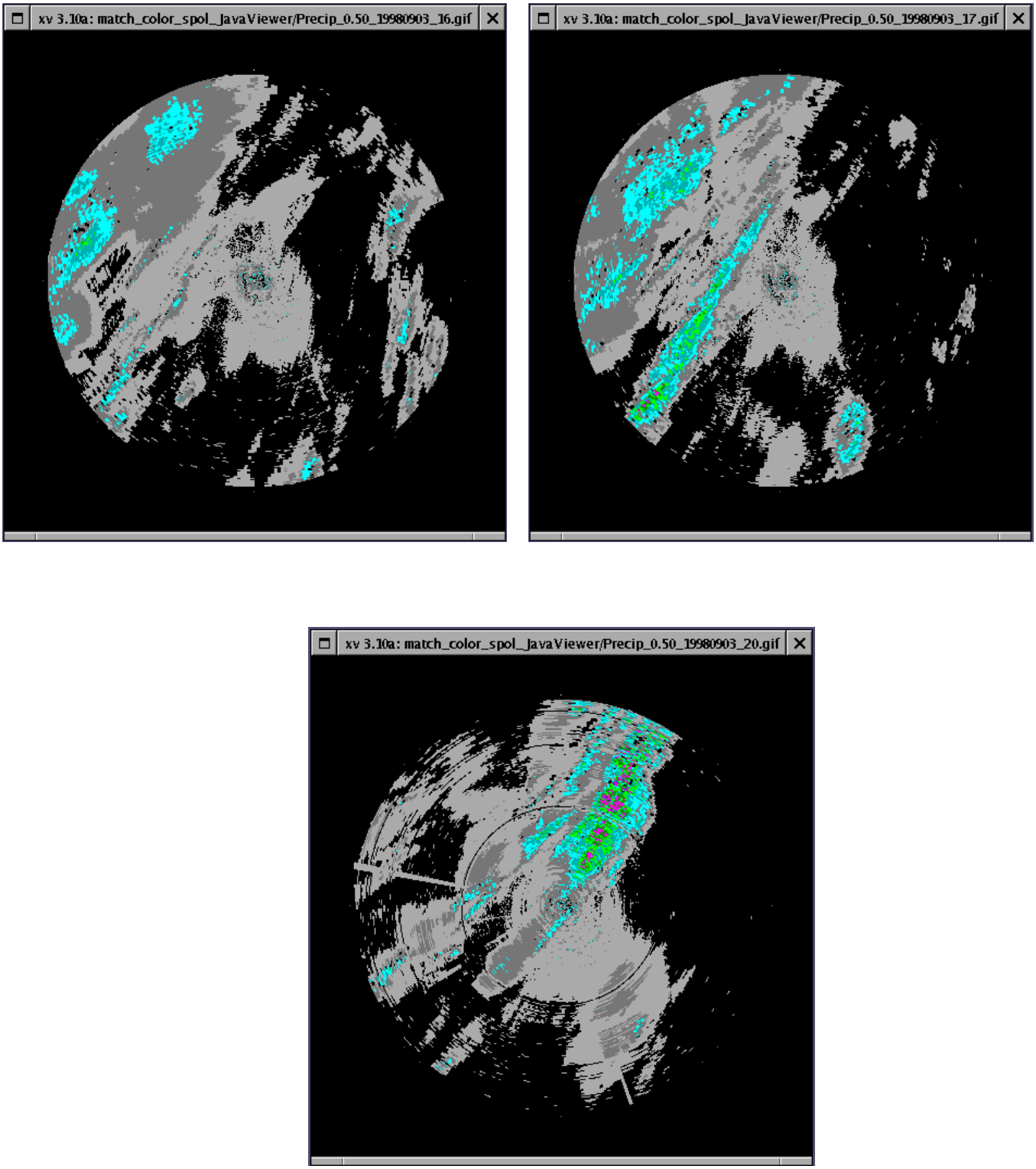

Figure 23. One-hour precipitation estimates derived from NCAR S-pol observations near Melbourne, Florida. Outer edge of coverage is 175 km range. Observations are from 3 September 1998, hourly periods ending (a) 1600 UTC, (b) 1700 UTC, and (c) 2000 UTC.

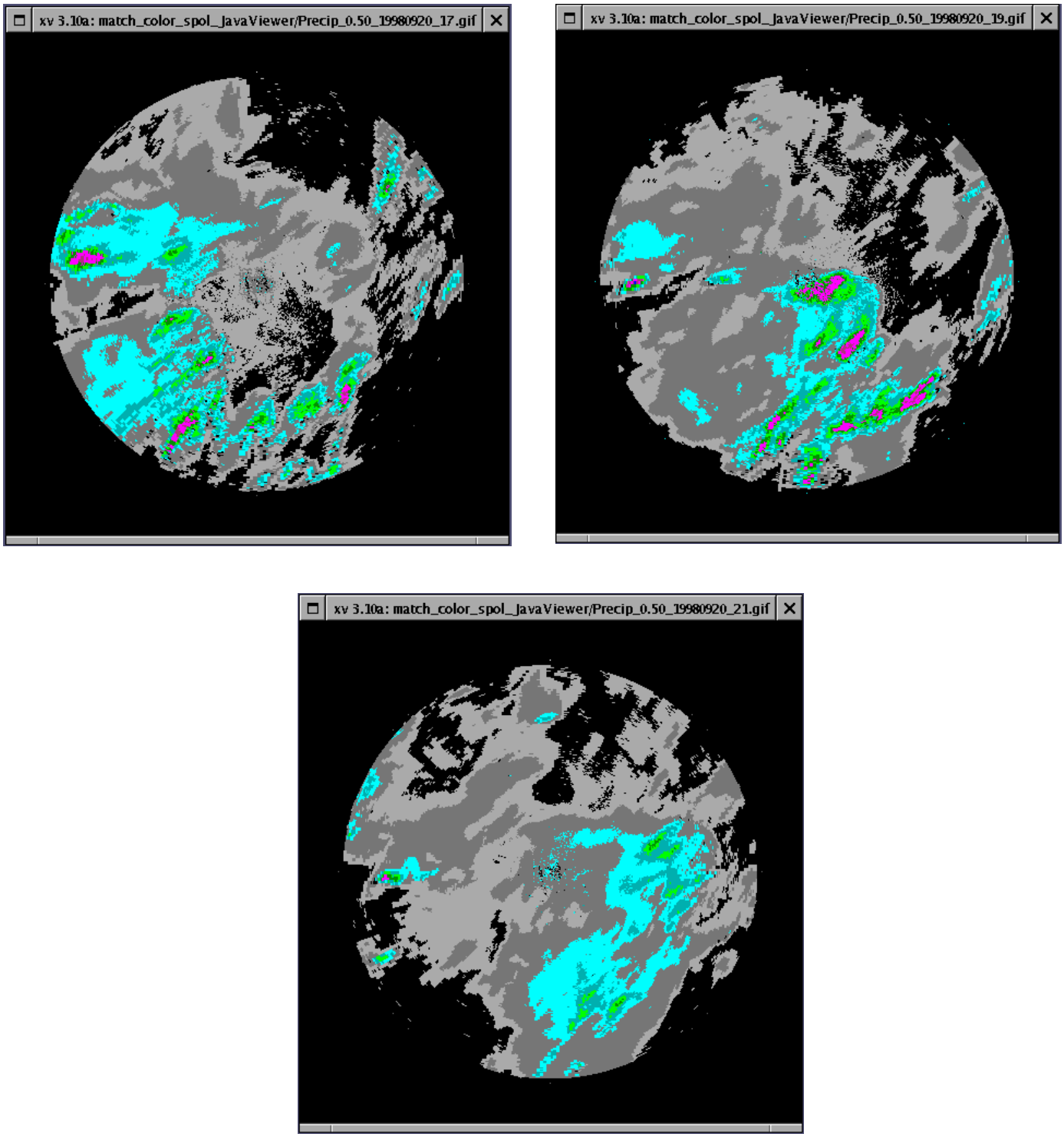

Figure 24. As in Fig. 18, except observations are from 21 September 1998, hourly periods ending (a) 1700 UTC, (b) 1900 UTC, and (c) 2100 UTC.

IV. Effects Of Beam Splitting On Precipitation Products

The planned implementation of polarimetric WSR-88D includes the use of a "beam splitting" strategy to enable the radar to simultaneously transmit vertically- and horizontally-polarized radiation. This feature enables the use of powerful dual-polarization moments including the reflectivity cross-correlation coefficient (Melnikov 2004). However, the effective splitting of the beam reduces the sensitivity of the radar by a small amount. This loss of sensitivity has the effect of eliminating some low-intensity echoes that might have been identified above the reflectivity noise level by the current WSR-88D processing system.

Initial estimates of the effects on derived products other than precipitation were made by Scharfenberg et al. (2005), who found some loss of information in the velocity products and near-negligible effects on 4-bit reflectivity products designed for graphical interpretation. They concluded that operational effects should be negligible. Their experiment was carried out by artificially degrading existing base data from the WSR-88D.

We will repeat the experiment of Scharfenberg et al. for digital precipitation products during the FY2007 cycle. However, we made some initial assessment of the differences in precipitation detection by the KOUN and KTLX radars. It must be kept in mind that any two WSR-88D units will exhibit differences in sensitivity if only through differences in electronics calibration. Furthermore, the precipitation and associated preprocessing algorithms are different. Therefore we can make only general conclusions from this experiment.

As noted earlier (and shown in Fig. 25) both the KOUN and KTLX units detected less measurable precipitation than was indicated by the Mesonet gauges – 36% of gauges showed precipitation while the corresponding KTLX estimates indicated 27% and KOUN, 24% coverage. The KTLX unit indicated slightly more measurable precipitation than did KOUN. Within the inner umbrella differences between KOUN and KTLX were very small, both indicating coverage of 32%.

In terms of the probability of detecting precipitation (finding the percentage of gauge report ≥ 0.01 inch that fell within the radar-indicated 0.01-inch isohyet), it appears that over the entire common umbrella area, the KTLX products detected more precipitation and with greater skill. As shown in Fig. 25, the KTLX DPA product detected 66% of the gauge-observed precipitation while the KOUN products detected between 59% and 62%. Within the inner umbrella, however, detection differences nearly vanished, ranging from 74-76%.

These findings (though tentative) suggest that some radar or algorithm differences might affect interpretation of echoes at ranges beyond 120 km, in terms of precipitation rate. The two radar units and algorithm sets yield very comparable results closer to the radar. When carrying out future experiments on precipitation detection and estimation we will concentrate attention on radar estimates at longer ranges, where we found some potentially significant performance differences.

Acknowledgements

We are indebted to the staff of NSSL, particularly Alexander Ryzhkov, John Krause, and Terry Schuur, for providing data and guidance for our evaluation. The staff of the NCAR radar applications group, particularly Scott Ellis, have dedicated substantial effort in providing dual-polarization observations from the S-pol radar unit, and willingly assisting in decoding and reformatting tasks.

References

Melnikov, V. M., 2004: Simultaneous transmission mode for the polarimetric WSR-88D. NSSL report available through: http://cimms.ou.edu/~schuur/reports/SHV_statistics.pdf

NCAR, 1999: S-Pol PRECIP98 Florida 1998. Available through: http://www.atd.ucar.edu/rsf/PRECIP98/precip98_intro.htm

Ryzhkov, A. V., T. J. Schuur, D. W. Burgess, P. L. Heinselman, S. E. Giangrande, and D. S. Zrnic, 2005: The Joint Polarization Experiment. *Bull. Amer. Meteor. Soc.*, **86**, 809-824.

_____, 2006: Polarimetric algorithms for hydrometeor classification (HCA) and quantitative precipitation estimation (QPE). Presentation to NEXRAD Software Review Committee.

Scharfenberg, K. A., K. L. Elmore, E. Forren, V. Melnikov, D. S. Zrnic, 2005: Estimating the impact of a 3-dB sensitivity loss on WSR-88D data. *Preprints, 32nd Conf. on Radar Meteorology*, Albuquerque, NM, USA, Amer. Meteor. Soc., CD-ROM, P12R.9.

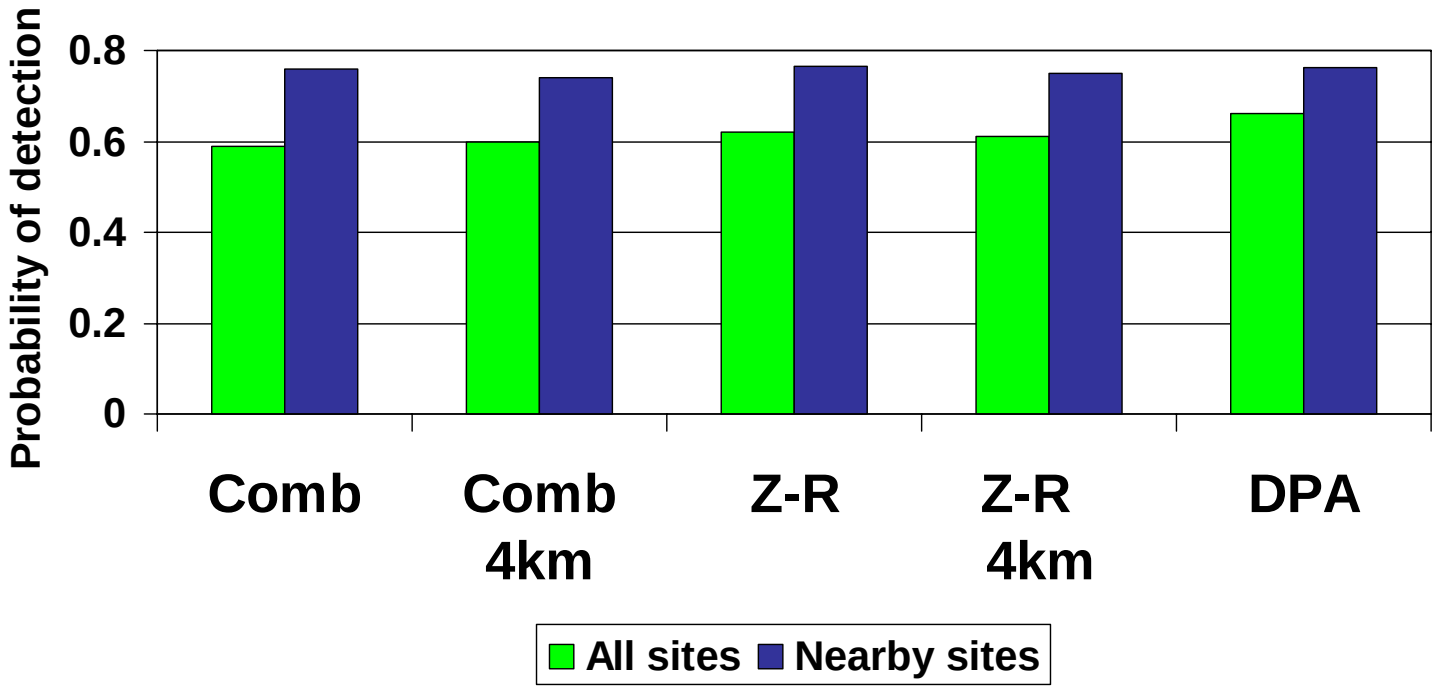

Figure 25. Probability of detecting 0.01 inches of precipitation as indicated by rain gauges, for all gauge sites in KOUN umbrella (green bars) and gauges within 120 km of the KOUN unit (blue bars).

OHD Publications Related To Radar And Multisensor Precipitation Algorithm Development

The publications below reflect other ongoing work in the Office of Hydrologic Development related to radar precipitation estimation. Those marked with an asterisk (*) are available through the Hydrometeorology Group web page at:

http://www.nws.noaa.gov/oh/hrl/papers/papers.htm#wsr88d

*Reed, S., R. Fulton, Z. Zhang, and S. Guan, 2006: Use of 4 km, 1 hr, precipitation forecasts to drive a distributed hydrologic model for flash flood prediction. *Preprints, 20th Conference on Hydrology*, San Diego, Amer. Meteor. Soc., J.84

*Ding, F., D. Kitzmiller, D. Riley, K. Shrestha, F. Moreda, and D.-J. Seo, 2005: Evaluation of the range correction algorithm and convective stratiform separation algorithm for improving hydrological modeling. *Preprints 32nd Conference on Radar Meteorology*, Albuquerque, Amer. Meteor. Soc., 13R.2.

*Guan, S., F. Ding, R. Fulton, and D. Kitzmiller, 2005: Preliminary results for the 0-1 hour Multisensor Precipitation Nowcaster. *Preprints 32nd Conference on Radar Meteorology*, Albuquerque, Amer. Meteor. Soc., 6R.4.

Kitzmiller, D., R. Fulton, S. Guan, F. Ding, W. Krajewski, G. Villarini, and G. Ciach, 2006: Development and planned operational applications of a conditional error model for radar rainfall estimates. Poster presentation, AGU Joint Assembly, Baltimore, H23B-02.

*Fulton, R., D. Kitzmiller, and J. Breidenbach, 2005: Multisensor Precipitation Estimator (MPE) Training Workshop (12/2005). Class lectures for National Weather Service Training Center Advanced Hydrologic Applications Course, December 2005.